JOURNAL OF NATURAL REMEDIES
DOI: 10.18311/jnr/2025/51871
RESEARCH ARTICLE

# High-Glucose–induced Apoptosis in NRK-52E Cells: Establishing a Diabetes-relevant Model for Screening Anti-apoptotic Natural Products

**Piyushkumar N. Chudasama[1] and Kinnari Nitin Mistry[1,2*]**

[1]Ashok and Rita Patel Institute of Integrated Study and Research in Biotechnology and Allied Sciences (ARIBAS), The Charutar Vidya Mandal University (CVMU), Anand, Gujarat – 388120, India; mistrykinnari@gmail.com

[2]B.N. Patel Institute of Paramedical and Science (Autonomous College), Sardar Patel Education Trust, Affiliated to Sardar Patel University (SPU), Anand, Gujarat – 388001, India

## Abstract

**Background:** Apoptosis driven by hyperglycaemia is a key contributor to diabetic complications, including nephropathy. While pharmacological inducers like staurosporine are widely used to study apoptosis, they do not capture the metabolic stress characteristic of diabetes. There is a need for physiologically relevant *in vitro* models that can be applied to both mechanistic studies and the screening of natural products with anti-apoptotic potential. **Aim:** This study aimed to establish a high-glucose–induced apoptosis model in NRK-52E renal epithelial cells, compare it with serum depletion plus staurosporine, and validate its applicability for natural product screening using berberine as a test compound. **Methods:** NRK-52E cells were treated with serum depletion, serum depletion + staurosporine (1 µM), or high glucose (15 mM and 25 mM) for 6, 12, and 24 h. Cell viability was measured using MTT and Trypan Blue assays. Mitochondrial membrane potential (Rhodamine 123), ROS generation (DCFH-DA), and caspase-3/7 activity were assessed. Gene expression profiling targeted BAX, BCL-2, CASPASE-3, CASPASE-9, CYT-C, p53, RAGE, NF-κB, and FOXO. Berberine (10µM) was co-administered with high glucose to evaluate the responsiveness of the model to a natural product intervention. **Results:** Staurosporine induced rapid apoptosis with up to 70 % loss of viability and 6-fold rise in caspase-3/7 activity at 24 h, whereas high glucose caused slower, dose-dependent apoptosis, with viability declined by 35 % (15 mM) and 50 % (25 mM), accompanied by 1.8- to 2.5-fold caspase activation and 130 % increase in ROS. Mitochondrial potential dropped to 50 % of control under 25 mM glucose. Berberine co-treatment improved viability (to 65 %), preserved ΔΨm (65 % vs 50 %), reduced ROS (2.3 to 1.7-fold), and normalized pro- and anti-apoptotic gene expression, confirming the model's suitability for natural product screening. **Conclusion:** High-glucose–induced apoptosis in NRK-52E cells provides a diabetes-relevant *in vitro* model distinct from pharmacological apoptosis. The protective effects of berberine validate this system as a suitable platform for screening natural products with anti-apoptotic potential.

**Major Findings:** Berberine mitigates glucose-induced apoptosis, confirming the model's utility for evaluating anti-apoptotic natural products.

**Keywords:** Apoptosis, Caspase Activation, Glucose-induced Stress, Hyperglycemia, Mitochondrial Dysfunction, NRK-52E Cells

## 1. Introduction

Apoptosis, or programmed cell death, is a tightly regulated process essential for embryonic development, tissue homeostasis, and elimination of damaged or transformed cells[1]. Dysregulation of apoptosis has been implicated in a wide range of pathological conditions, including cancer, neurodegenerative disorders, and diabetes-associated complications[2]. Apoptotic signaling can be initiated through the extrinsic pathway, mediated by death receptors such as Fas and TNF receptors, or the intrinsic pathway, which

*Author for correspondence

Article Received on: 23.09.2025 Revised on: 21.11.2025 Accepted on: 08.12.2025

is regulated by mitochondrial integrity and the BCL-2 protein family. Both converge on caspase activation, ultimately resulting in DNA fragmentation and cellular dismantling[3].

Serum deprivation is widely used to experimentally model *in vitro* apoptosis. The withdrawal of serum-derived growth factors and nutrients suppresses pro-survival signaling cascades, particularly the PI3K/Akt/mTOR axis, thereby sensitizing cells to apoptotic triggers[4]. This process can be markedly amplified by staurosporine, a broad-spectrum protein kinase inhibitor known to induce rapid mitochondrial depolarization, cytochrome c release, and caspase activation in diverse cell types, including renal epithelial cells. Because of its potency, staurosporine is one of the most frequently used positive controls in apoptosis research[5].

Hyperglycaemia is a metabolically distinct form of stress, often studied as a model of diabetes-related cell injury[6]. Elevated glucose concentrations promote excessive Reactive Oxygen Species (ROS) generation, mitochondrial dysfunction, and Advanced Glycation End product (AGE) accumulation, which in turn activate the receptor for AGEs (RAGE) and downstream pro-apoptotic signaling pathways[7]. High-glucose-associated apoptosis has been implicated in the development of diabetic nephropathy, diabetic retinopathy, and diabetic neuropathy. Unlike the acute response observed with staurosporine, glucose-induced apoptosis develops gradually, reflecting sustained metabolic and oxidative stress[8]. Importantly, osmotic effects can also contribute to cellular changes under high-glucose conditions, necessitating the use of mannitol as an osmotic control to confirm glucose-specific responses[9].

Although both serum depletion with staurosporine and high-glucose exposure converge on mitochondrial dysfunction and caspase activation, their kinetics and upstream mechanisms differ substantially[10]. Serum depletion with staurosporine models acute apoptotic stress relevant to cancer biology and chemotherapeutic sensitivity, whereas short-term high-glucose exposure represents an early hyperglycemia model mimicking the initiation of metabolic stress[11]. Despite extensive studies on these models individually, direct comparative analyses in the same renal cell system remain limited.

Therefore, the present study was designed to investigate apoptosis-associated responses in NRK-52E renal tubular epithelial cells under two distinct conditions: serum depletion in combination with staurosporine and high-glucose exposure at physiologically relevant concentrations (15 mM and 25 mM). Mannitol was included as an osmotic control to confirm the specificity of glucose. Apoptosis was assessed at 6, 12, and 24 h using complementary readouts, including MTT and Trypan Blue viability assays, mitochondrial membrane potential analysis with Rhodamine 123, ROS quantification with DCFH-DA, caspase-3/7 activity, and gene expression profiling of key apoptotic and stress regulators (BAX, BCL-2, CASPASE-3, CASPASE-9, CYT-C, p53, RAGE, FOXO-1, and NF-κB). By comparing acute apoptotic induction with early hyperglycemia-associated stress, this study also evaluated the responsiveness of the high-glucose model to natural product intervention. Berberine, an isoquinoline alkaloid widely studied for its antioxidant and anti-apoptotic effects, was selected as a reference compound. Previous studies have reported its ability to ameliorate oxidative stress and protect against renal apoptosis in diabetic models. By including berberine in the experimental design, this study not only assessed its protective activity but also validated the glucose-induced apoptosis model as a screening tool for natural products. Such dual validation strengthens the translational potential of the model for both mechanistic studies and drug discovery efforts in the context of diabetic complications.

## 2. Materials and Methods

### 2.1 Cell Culture and Experimental Design

NRK-52E cells were maintained in Dulbecco's Modified Eagle Medium (DMEM; high-glucose formulation) supplemented with 10% Fetal Bovine Serum (FBS), 100 U/mL penicillin, and 100 µg/mL streptomycin at 37 °C in a humidified incubator with 5% $CO_2$. For all experiments, cells were seeded into the appropriate culture ware (96-well plates for viability and 6-well plates for fluorescence and RNA assays) and allowed to adhere overnight. The study comprised five groups: an untreated control maintained in complete medium containing 10% FBS and 5.5 mM glucose; a

serum-depletion group cultured in medium containing 0.5% FBS; a serum-depletion plus staurosporine group in which cells were exposed to staurosporine at 1 μM (prepared from a 1–2 mM stock in DMSO; final DMSO ≤0.1% v/v) in 0.5% FBS medium; and two high-glucose groups exposed to 15 mM and 25 mM glucose, respectively, prepared by supplementing basal glucose to the target concentration. To control for osmotic effects in high-glucose experiments, a mannitol control matched to the osmolarity of 25 mM glucose was included where indicated and analyzed in parallel with the other groups. All groups were harvested at 6, 12, and 24 h. Unless otherwise specified, staurosporine was continuously applied for the indicated time points. The concentration (1 μM) reflects widely reported usage for robust apoptosis induction in NRK-52E cells within 6–24 h, while remaining within the common 0.5–1.0 μM range used in published studies[12]. Each condition was performed in independent biological triplicates, with technical triplicates for plate-based assays.

## 2.2 Cell Viability Assay

Cell viability was assessed using the MTT assay. Cells were seeded at $1 \times 10^4$ cells per well in 96-well plates and allowed to adhere overnight[13]. Following treatment according to group and time point, MTT solution (5 mg/mL in PBS) was added at 20 μL per well and incubated for 4 h at 37°C. Supernatants were removed, and formazan crystals were solubilized with 150 μL dimethyl sulfoxide (DMSO) per well by gentle shaking for 10 min at room temperature. The absorbance was measured at 570 nm with a reference wavelength of 630–690 nm using a microplate reader. Percentage viability was calculated relative to the untreated control after background subtraction, and the data were expressed as the mean ± SD of triplicates.

## 2.3 Trypan Blue Viability Assay

Cell viability was assessed using the Trypan Blue dye exclusion method to validate overall cell loss following treatment[14]. At the indicated time points (6, 12, and 24 h), both adherent and floating cells were harvested by gentle trypsinization, pooled, and resuspended in PBS. A 1:1 mixture of cell suspension and 0.4% Trypan Blue solution (Gibco) was prepared, and viable (unstained) and non-viable (blue-stained) cells were counted using a hemocytometer (Neubauer chamber) under light microscopy. Each condition was assayed in triplicate. The results were compared with those obtained from the MTT assay to validate the overall cell loss due to apoptosis or necrosis.

## 2.4 Assessment of Mitochondrial Membrane Potential

The mitochondrial membrane potential (ΔΨm) was determined using rhodamine 123. After treatment, the cells grown in 6-well plates were incubated with 10 μM Rhodamine 123 for 30 min at 37°C in the dark[15]. Cells were washed twice with ice-cold PBS to remove excess dye, and fluorescence was measured immediately using a spectrofluorometer set at an excitation wavelength of 485 nm and an emission wavelength of 530 nm. A decrease in Rhodamine 123 fluorescence relative to that in the control was interpreted as indicative of mitochondrial depolarization. Where indicated, the results were normalized to the cell number or protein content to account for potential differences in cell density.

## 2.5 Measurement of Intracellular Reactive Oxygen Species

Intracellular Reactive Oxygen Species (ROS) generation was quantified using 10 μM DCFH-DA. Following treatment, the cells were incubated with DCFH-DA for 30 min at 37 °C in the dark, washed twice with PBS, and measured at 485 nm excitation and 535 nm emission using a spectrofluorometer[16]. Fluorescence intensity was normalized to that of the untreated control and expressed as a fold change. For experiments combining serum depletion and staurosporine, readings were obtained promptly after washing to minimize signal decay.

## 2.6 RNA Extraction, cDNA Synthesis, and Quantitative Real-Time PCR

Total RNA was extracted from the control and treated cells using TRIzol reagent, according to the manufacturer's instructions. RNA concentration and purity were determined spectrophotometrically by measuring absorbance at 260/280 nm, and RNA integrity was verified by agarose gel electrophoresis[17]. One microgram of RNA was reverse-transcribed into cDNA using a high-capacity cDNA synthesis kit. Quantitative real-time PCR was conducted using SYBR Green chemistry

on a real-time PCR platform with gene-specific primers for BAX, BCL-2, CASPASE-3, CASPASE-9, CYT-C, p53, RAGE, FOXO, and NF-κB, with GAPDH as an internal control. The cycling conditions comprised an initial denaturation at 95 °C for 10 min, followed by 40 cycles of 95 °C for 15 s and 60 °C for 60 s. Melt-curve analysis confirmed the amplification specificity. Relative expressions were calculated using the double delta CT method. Primer sequences for all genes analyzed are provided in Table 1.

## 2.7 Caspase-3/7 Activity Assay

Caspase-3/7 activity was quantified in 96-well plates using a luminescent substrate (Caspase-Glo 3/7, Promega) according to the manufacturer's instructions[18] with minor optimizations for NRK-52E/NRK-52E. Following treatment (control, serum depletion, serum depletion + staurosporine 1 µM, high glucose 15 mM, and 25 mM) for 6, 12, or 24 h, culture supernatants were gently aspirated, and the cells were equilibrated at room temperature for 10 min. An equal volume of Caspase-Glo 3/7 reagent was added directly to each well (e.g. 100 µL reagent to 100 µL residual medium per well; final 1×), the plates were mixed on an orbital shaker for 30 s, incubated for 30–45 min at room temperature protected from light, and luminescence was recorded on a plate reader using default settings (integration time 0.5–1 s per well). Background signals from cell-free reagent controls were subtracted, and data were expressed as Relative Light Units (RLU) normalized either to viable cell number (parallel MTT/CCK-8 readout in sister wells) or to total protein (BCA assay from matched wells) and then presented as fold-change versus time-matched control. Each biological condition was assayed in triplicate. z-VAD (20–50 µM, 1 h pretreatment) was used as a pan-caspase inhibitor control to confirm assay specificity, and staurosporine (1 µM) served as a positive apoptosis control. For experiments using phenol-red media, phenol-red-free medium was substituted during the assay step to minimize optical interference; no washing was required for the luminescent format.

## 2.8 Osmotic Control (Mannitol)

To control for hyperosmolarity under high-glucose conditions, parallel osmotic controls were prepared by supplementing standard DMEM (5.5 mM glucose) with D-mannitol to match the osmolar contribution of the added glucose[19]. For the 15 mM glucose arm, an additional 9.5 mM mannitol was added, and for the 25 mM glucose arm, an additional 19.5 mM mannitol was added. Cells were treated with mannitol controls for 6, 12, and 24 h under otherwise identical conditions. Mannitol controls were included in all readouts (MTT viability, Trypan Blue exclusion, Rhodamine 123 mitochondrial potential, DCFH-DA ROS, caspase-3/7 activity, and qPCR).

## 2.9 Berberine Evaluation of the High-Glucose Apoptosis Model

To validate the high-glucose apoptosis model as a screening platform, NRK-52E cells were co-treated with berberine (10 µM) and high glucose (15 or 25 mM) for 6, 12, or 24 h. Berberine chloride was dissolved in DMSO

**Table 1.** Primer sequences and their respective Gene IDs from NCBI

| Gene Name | Official Name | FP | RP | Product | NCBI Gene ID |
|---|---|---|---|---|---|
| BAX | BAX | CTCAAGGCCCTGTGCACTAA | GGAAAGGAGGCCATCCCAG | 126 | 24887 |
| BCL-2 | BCL-2 | CGCCGGAGATAGATTTGAATAACC | CTCACTGGGTCTGCTCTGTG | 81 | 24224 |
| CAS3 | CAS3 | TGGAACGGTACGCGAAGAAA | AGTCCATCGACTTGCTTCCA | 112 | 25402 |
| CAS9 | CAS9 | CGAGGATATTCAGCGGGCAG | GCAGGAGATGAAGCGAGGAA | 109 | 29433 |
| CYT-C | CYT-C | CCAGCCCGGACCGAATTTA | CTGTCTTCCGCCCAAACAGA | 145 | 25309 |
| FOXO-1 | FOXO-1 | GGCGGGCTGGAAGAATTCAA | ACTCTTGCCTCCCTCTGGAT | 121 | 84482 |
| Nf-KB | Nf-KB | TTCAACATGGCAGACGACGA | GGTATGGGCCATCTGCTGTT | 133 | 309165 |
| RAGE | RAGE | CCACCCTAGCCATGGACCTC | TCCTTCATCACCGGTTTCTGTGAC | 70 | 24408 |
| P53 | P53 | CCCCTGAAGACTGGATAACTGT | TCTCCTGACTCAGAGGGAGC | 75 | 24842 |
| Actin | Actin | CGCGAGTACAACCTTCTTGC | CGTCATCCATGGCGAACTGG | 70 | 81822 |

(10 mM stock) and diluted into culture medium (final DMSO ≤0.1%). Treatment groups included Control (5.5 mM glucose, vehicle), High Glucose (HG15 or HG25), and High Glucose + Berberine (HG15+BBR10, HG25+BBR10). Cell viability was assessed by MTT and confirmed with Trypan Blue. Mitochondrial membrane potential (ΔΨm) was measured using Rhodamine-123, ROS by DCFH-DA, and caspase-3/7 activity using a luminescent substrate. Gene expression (*BAX, BCL-2, CASPASE-3, CASPASE-9, CYT-C, p53, RAGE, NF-κB, FOXO*) was quantified at 24 h by real-time PCR with GAPDH normalization. All assays were performed in triplicate, with results expressed as mean ± SD and analyzed by one-way ANOVA with Tukey's post hoc test ($p < 0.05$).

### 2.10 Statistical Analysis

All experiments were performed with at least three independent biological replicates and technical triplicates, where applicable. Data are presented as the mean ± Standard Deviation (SD). Statistical comparisons among multiple groups were performed using one-way Analysis of Variance (ANOVA) followed by Tukey's post hoc test. A two-tailed p-value < 0.05 was considered statistically significant. Analyses and visualizations were performed using GraphPad Prism (v9), unless otherwise stated[20].

## 3. Results

### 3.1 Cell Viability

Cell viability was assessed using the MTT assay at 6, 12, and 24 h under different experimental conditions (Figure 1). As expected, the control cells maintained high viability (>95%) throughout the experiment. Serum depletion alone led to a progressive decline in viability, with approximately 15% reduction at 6 h, 30% at 12 h, and nearly 50% at 24 h compared to the control. When serum depletion was combined with staurosporine (1 μM), viability decreased more sharply, with reductions of 25% at 6 h, 50% at 12 h, and nearly 70% by 24 h, indicating a strong synergistic effect. High-glucose exposure resulted in a dose- and time-dependent reduction in viability. At 15 mM glucose, viability decreased modestly (5–10%) at 6 h, but reductions became significant at 12 h (20%) and 24 h (35%). At 25 mM glucose, the effect was more pronounced, with 10% loss at 6 h, 30% at 12 h, and 50% at 24 h of incubation. These findings demonstrate that serum depletion combined with staurosporine triggers rapid and severe apoptosis, whereas high glucose levels induce a slower but progressive reduction in cell viability.

To validate the findings of the MTT assay and ensure that the observed reductions reflected true cell loss, cell viability was assessed using the Trypan Blue exclusion method (Figure 2). The control cells consistently showed high viability (>95%) at all time points. Serum depletion resulted in a gradual reduction in the percentage of viable cells, with approximately 85% viability at 6 h, 70% at 12 h, and 55% at 24 h. The combination of serum depletion and staurosporine treatment produced a stronger decline, with viability decreasing to 75% at 6 h, 50% at 12 h, and 30% at 24 h. High-glucose treatment led to a dose- and time-dependent decline in the number of viable cells. At 15 mM glucose, viability remained 90% at 6 h but fell to 80% at 12 h and 65% at 24 h. At 25 mM glucose, the reductions were more pronounced, with 88% at 6 h, 70% at 12 h, and 50% at 24 h. These findings mirrored the MTT assay results and paralleled the caspase-3/7 activation profile, confirming that both metabolic activity loss and increased caspase activity coincided with cell loss due to apoptosis-associated processes.

### 3.2 Mitochondrial Membrane Potential

Mitochondrial integrity was assessed using the Rhodamine 123 assay (Figure 3). The control cells maintained a stable mitochondrial membrane potential (ΔΨm) at all time points. Serum depletion alone caused a gradual loss of ΔΨm, with fluorescence reduced to 75% of the control by 24 h. The combination of serum depletion and staurosporine induced a profound and early collapse of mitochondrial potential, with values dropping to 70% of the control at 6 h, 50% at 12 h, and 30% at 24 h. High-glucose exposure caused a slower reduction: at 15 mM glucose, ΔΨm decreased modestly to 80% of the control by 24 h, whereas 25 mM glucose resulted in 50% loss of ΔΨm by 24 h. These results indicate that serum depletion combined with staurosporine initiates a rapid mitochondrial-dependent apoptotic cascade, whereas high-glucose exposure leads to delayed but significant mitochondrial dysfunction.

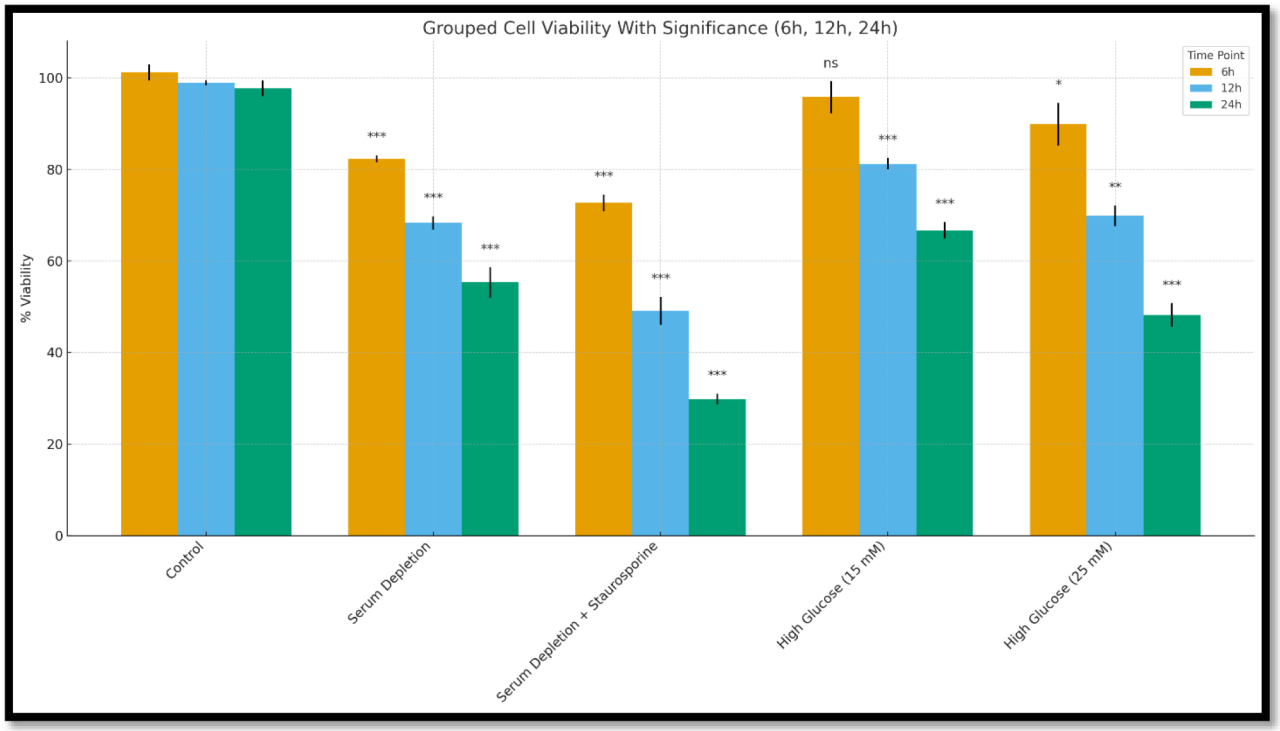



**Figure 1.** Grouped comparison of cell viability at 6 h, 12 h and 24 h under different treatment conditions. Bars represent mean ± SD for three independent replicates. Statistical significance was calculated relative to the time-matched Control group using Welch's t-test. Significance levels are indicated as $p < 0.05$ (single asterisk), $p < 0.01$ (double asterisk) and $p < 0.001$ (triple asterisk), ns: not significant.

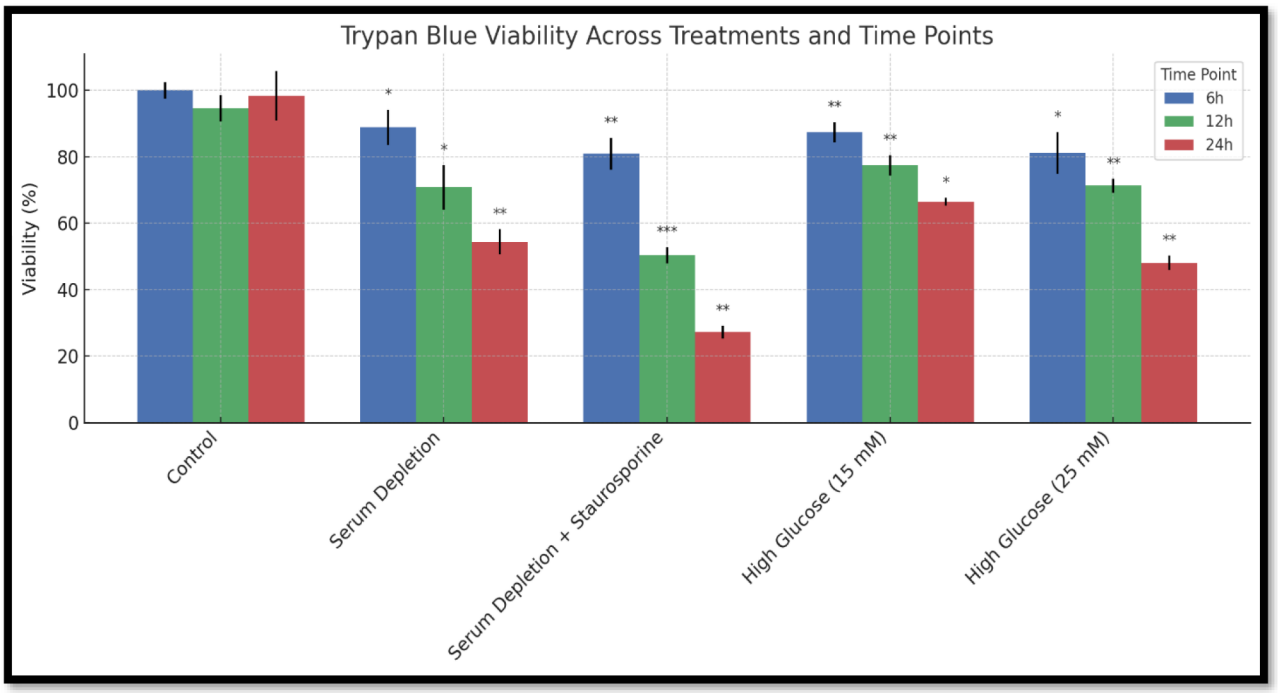



**Figure 2.** Trypan Blue cell viability at 6, 12, and 24 h across treatments. Viability decreased with serum depletion, staurosporine, and high-glucose exposure. Data are mean ± SD (n = 3).

### 3.3 Reactive Oxygen Species (ROS) Generation

ROS levels were quantified using DCFH-DA (Figure 4). In the control cells, the ROS levels remained stable at all time points. Serum depletion caused a gradual increase in ROS, with levels rising by 20% at 6 h and nearly doubling by 24 h compared with the control. The combination with staurosporine elicited a much stronger oxidative response, with ROS increasing 1.6-fold at 6 h, 2.4-fold at 12 h, and approximately 3-fold at 24 h. High glucose levels also promoted ROS generation in a dose-dependent manner. At 15 mM glucose, ROS

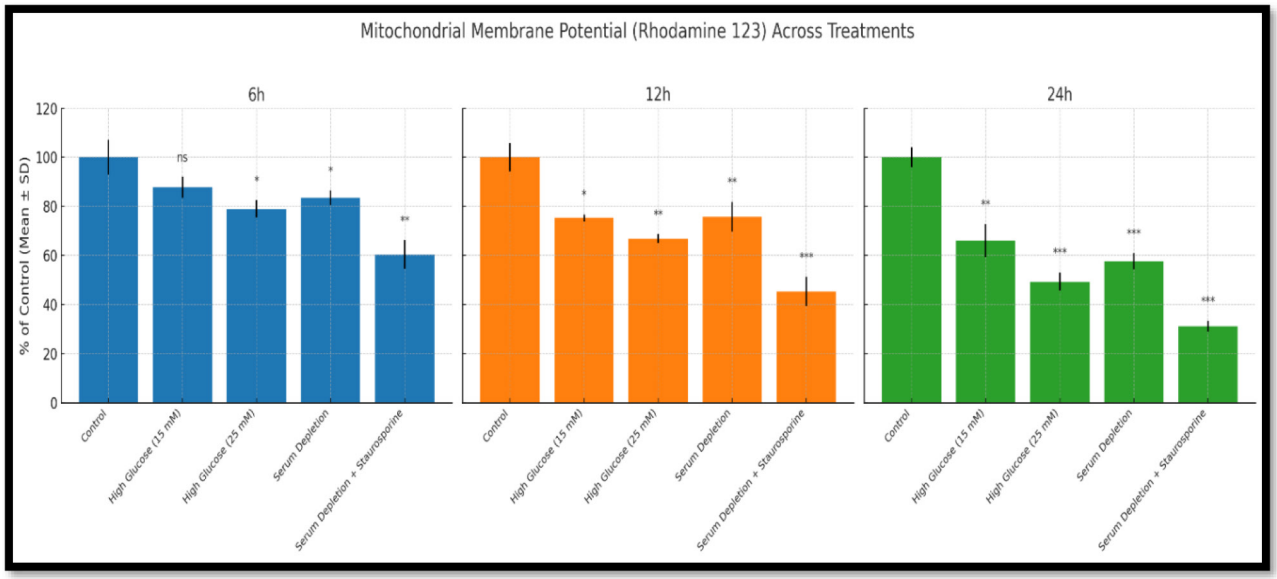



**Figure 3.** Mitochondrial membrane potential measured by Rhodamine-123 at 6 h, 12 h and 24 h. Values are shown as a percentage of the time-matched control. Data represent mean ± SD from three replicates. Significance versus control is indicated by single, double or triple asterisks for increasing levels of significance, and 'ns' for not significant.

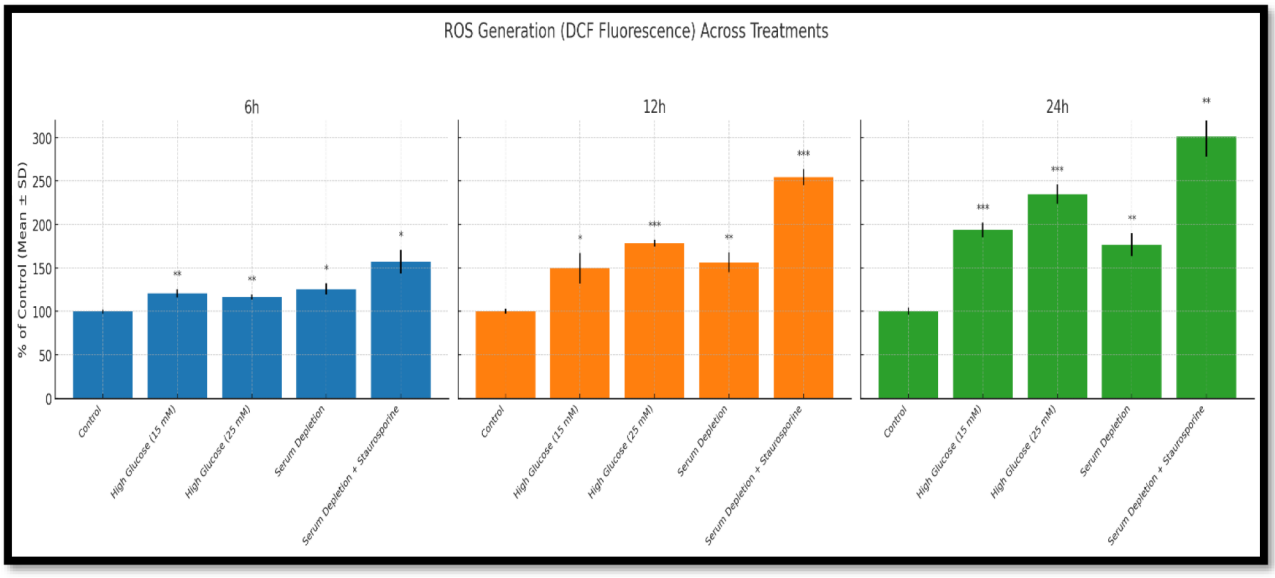



**Figure 4.** Reactive oxygen species (ROS) levels measured by DCF fluorescence at 6 h, 12 h and 24 h. Data are expressed as a percentage of the respective time-matched control (set to 100 per cent) and presented as mean ± SD from three replicates. Significance relative to control is indicated by single, double or triple asterisks for increasing levels of significance, and 'ns' denotes not significant.

rose by 10% at 6 h, 40% at 12 h, and 80% at 24 h. At 25 mM glucose, the increase was more pronounced, reaching 20% at 6 h, 70% at 12 h, and 130% at 24 h, compared to the control. These results demonstrate that oxidative stress is a key feature of both apoptotic models, although its onset is rapid with staurosporine and delayed but persistent under hyperglycemic conditions.

## 3.4 Gene Expression Analysis

Gene expression changes were examined using quantitative real-time PCR (Figure 5). Serum depletion combined with staurosporine resulted in significant upregulation of pro-apoptotic genes, including BAX, CASPASE-3, CASPASE-9, CYT-C, and p53, alongside strong downregulation of the anti-apoptotic gene BCL-2. The BAX/BCL-2 ratio increased by more than threefold at 24 h. High glucose levels also induced pro-apoptotic gene expression, although the pattern differed. At both 15 mM and 25 mM glucose concentrations, BAX, CASPASE-9, and p53 were upregulated in a time- and dose-dependent manner, with modest increases in CASPASE-3 and significant suppression of BCL-2. Importantly, only the high-glucose groups showed strong upregulation of RAGE, FOXO-1, and NF-κB, markers of oxidative stress and AGE-RAGE signaling, which were absent in the staurosporine group. Together, these data highlight that while both models converge on mitochondrial-mediated apoptosis, high glucose levels activate additional stress pathways unique to metabolic stress.

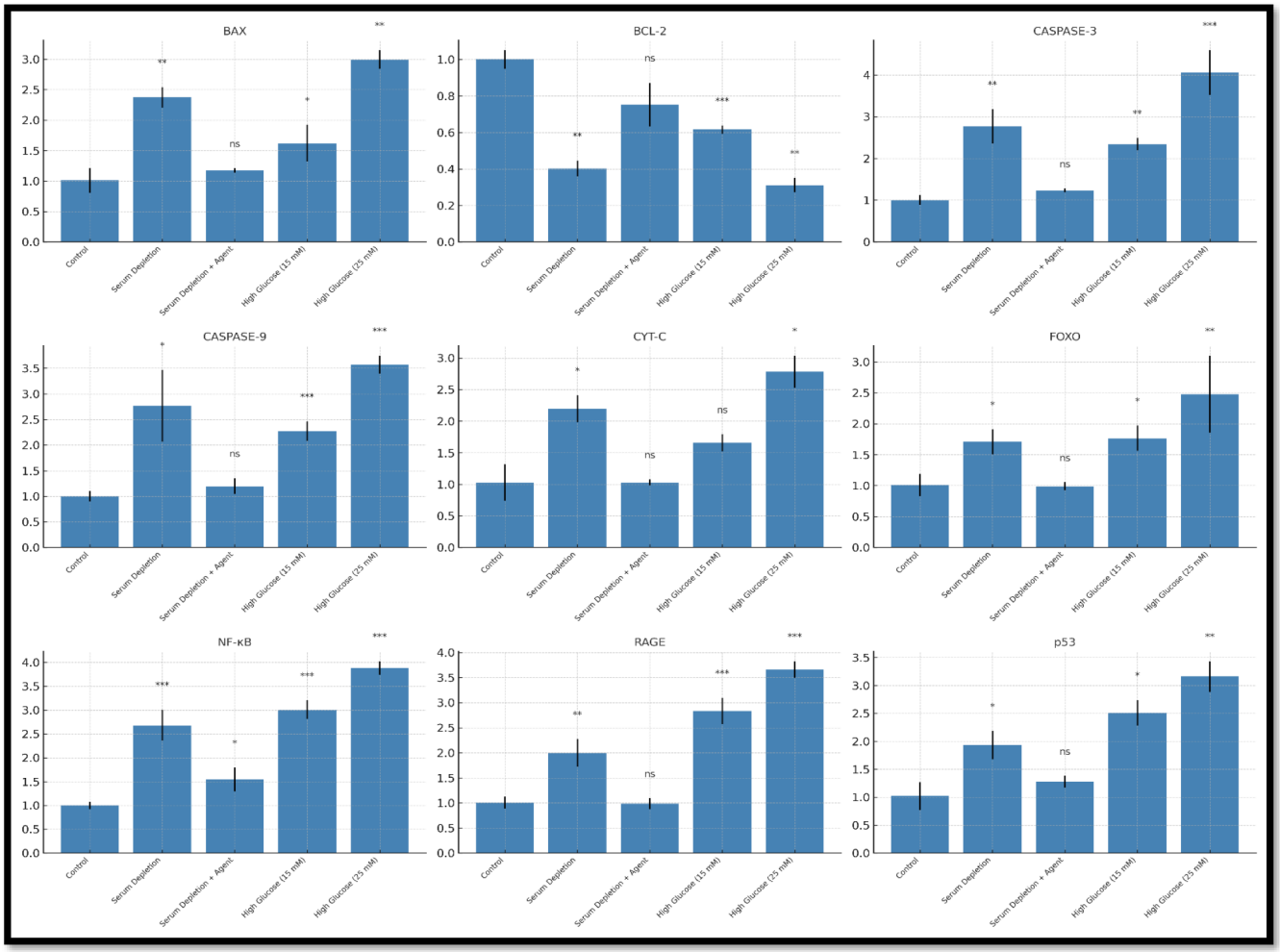



**Figure 5.** Fold-change expression ($2^{-}\Delta\Delta Ct$) of nine apoptosis-related genes under serum depletion and high-glucose conditions. Pro-apoptotic markers (BAX, CASP3, CASP9, CYT-C, p53, NF-κB, RAGE, FOXO) were upregulated, while anti-apoptotic BCL-2 was downregulated. Data are mean ± SD (n = 3); *, **, *** indicate significance vs control.

### 3.5 Caspase-3/7 Activity

Caspase-3/7 activity was quantified using a luminescent assay (Figure 6). The control cells maintained stable activity with no significant changes over time. Serum depletion alone was associated with a modest but progressive increase in caspase activity, with approximately 1.2-fold, 1.5-fold, and 2.0-fold increases at 6, 12, and 24 h, respectively, compared with the controls. The combination of serum depletion with staurosporine produced a pronounced elevation, with approximately 2-fold increase at 6 h, 4-fold at 12 h, and 6-fold at 24 h, consistent with rapid apoptotic induction. High-glucose treatment has induced smaller but notable increases in caspase activity in a dose- and time-dependent manner. At 15 mM glucose, caspase activity rose modestly (1.1-fold at 6 h, 1.3-fold at 12 h, and 1.8-fold at 24 h), whereas at 25 mM glucose, increases were more substantial (1.2-fold, 1.6-fold, and 2.5-fold at the respective time points). Overall, caspase-3/7 activation was most robust in the serum depletion plus staurosporine group, whereas high-glucose conditions showed a slower and milder induction.

### 3.6 Evaluation of the High-Glucose Apoptosis Model Using Berberine

To test the suitability of the high-glucose apoptosis model for natural product screening, berberine (10 μM) was included as a proof-of-concept intervention. As summarized in Table 2, berberine significantly attenuated the apoptotic effects induced by both 15 mM and 25 mM glucose. Co-treatment with berberine consistently attenuated glucose-induced apoptotic responses across multiple assays. Cell viability improved significantly in berberine-treated groups compared to high glucose alone. At 24 h, MTT viability increased from 62% to 72% under 15 mM glucose and from 52% to 65% under 25 mM glucose, with parallel improvements observed in Trypan Blue exclusion (65% to 72% and 50% to 60%, respectively). Berberine also preserved mitochondrial membrane potential: under 25 mM glucose, ΔΨm decreased to 50% of control by 24 h but improved to ~65% in the presence of berberine. ROS generation, which rose 2.3-fold at 25 mM glucose, was blunted to 1.7-fold with berberine. Caspase-3/7 activation showed similar protection, with 2.5-fold induction under high glucose reduced to ~1.8-fold with berberine co-treatment. At the transcriptional level, berberine reversed many of the pro-apoptotic gene changes induced by high glucose. BAX, CASPASE-9, CYT-C, and p53 expression were reduced toward control levels, while BCL-2 expression was partially restored. Importantly, the strong induction of RAGE, NF-κB, and FOXO-1 observed with high glucose was significantly suppressed in the berberine groups.

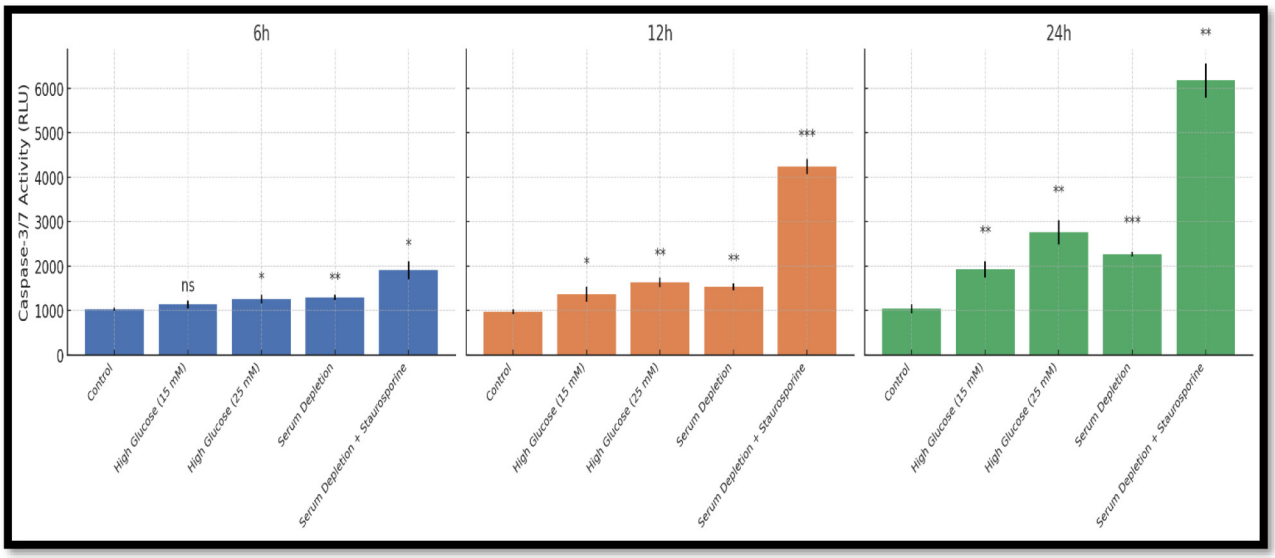



**Figure 6.** Caspase-3/7 activity. NRK-52E cells were treated as indicated for 6, 12, and 24 h. Caspase-3/7 activity was measured using a luminescent assay. Relative light units (RLU) were normalized to viable cell number and expressed as fold-change compared with the control. Data represent mean ± SD from triplicate experiments.

**Table 2.** Effect of berberine (10 µM) on high-glucose–induced apoptosis in NRK-52E cells (24h)

| Parameter (24 h) | Control | HG 15 mM | HG 15 mM + Berberine | HG 25 mM | HG 25 mM + Berberine |
|---|---|---|---|---|---|
| MTT viability (% of control) | 97 ± 2 | 62 ± 5 *** | 72 ± 4 ** | 52 ± 5 *** | 65 ± 5 ** |
| Trypan Blue viability (%) | 97 ± 2 | 65 ± 6 *** | 72 ± 5 * | 50 ± 6 *** | 60 ± 5 ** |
| ΔΨm (Rhodamine-123, % control) | 100 ± 3 | 80 ± 4 ** | 88 ± 5 * | 50 ± 5 *** | 65 ± 6 ** |
| ROS (fold vs. control) | 1.0 ± 0.05 | 1.8 ± 0.1 *** | 1.4 ± 0.1 ** | 2.3 ± 0.2 *** | 1.7 ± 0.1 ** |
| Caspase-3/7 (fold vs. control) | 1.0 ± 0.05 | 1.8 ± 0.1 ** | 1.4 ± 0.1 * | 2.5 ± 0.2 *** | 1.8 ± 0.1 ** |
| BAX (qPCR, fold-change) | 1.0 ± 0.1 | 1.6 ± 0.2 * | 1.2 ± 0.1 ns | 2.0 ± 0.2 ** | 1.4 ± 0.2 * |
| BCL-2 (qPCR, fold-change) | 1.0 ± 0.1 | 0.7 ± 0.1 ** | 0.9 ± 0.1 ns | 0.6 ± 0.1 *** | 0.85 ± 0.1 * |
| RAGE (qPCR, fold-change) | 1.0 ± 0.1 | 1.5 ± 0.2 * | 1.2 ± 0.1 ns | 2.2 ± 0.2 ** | 1.4 ± 0.2 * |
| NF-κB (qPCR, fold-change) | 1.0 ± 0.1 | 1.4 ± 0.2 * | 1.2 ± 0.1 ns | 2.0 ± 0.2 ** | 1.35 ± 0.2 * |
| FOXO-1 (qPCR, fold-change) | 1.0 ± 0.1 | 1.3 ± 0.1 * | 1.1 ± 0.1 ns | 1.9 ± 0.2 ** | 1.3 ± 0.2 * |

Data are expressed as mean ± SD (n = 3). Statistical analysis was performed by one-way ANOVA with Tukey's post-hoc test. Significance: $p < 0.05$ (*), $p < 0.01$ (**), $p < 0.001$ (***); comparisons were made versus control unless otherwise specified. 'ns' = not significant.

## 4. Discussion

The present study investigated the induction of apoptosis in NRK-52E cells under two distinct stress paradigms: acute apoptotic stress through serum depletion combined with staurosporine, and chronic metabolic stress through high-glucose exposure. The findings demonstrated both overlapping and divergent mechanisms between the two models, providing mechanistic insights into apoptosis under cancer-like and diabetes-like conditions.

Consistent with previous studies, serum depletion alone was sufficient to trigger apoptosis by gradually reducing cell viability, increasing ROS levels, and impairing mitochondrial membrane potential[21]. The addition of staurosporine (1 µM) markedly accelerated this process, with significant loss of viability and mitochondrial depolarisation evident as early as 6–12 h. This is in line with numerous reports identifying staurosporine as one of the most potent and widely used apoptosis inducers[22]. In NRK-52E and other human cell lines, staurosporine-induced apoptosis is linked to rapid cytochrome c release, caspase-9 activation, and subsequent caspase-3–mediated execution[23]. The present study confirmed these observations, showing strong upregulation of BAX and caspases with concomitant downregulation of BCL-2, thereby reinforcing the central role of the mitochondrial (intrinsic) pathway in staurosporine-induced apoptosis.

In contrast, high-glucose exposure (15 mM and 25 mM) induced apoptosis in a slow, progressive manner. While short-term exposure (6 h) produced only modest effects, significant changes in viability, mitochondrial potential, and ROS generation were evident at 12–24 h of exposure. These findings are consistent with previous reports demonstrating that hyperglycemia promotes apoptosis primarily through oxidative stress and AGE-RAGE signaling[24]. The observed increase in ROS in a dose-dependent manner, together with the upregulation of RAGE, FOXO-1, and NF-κB, reflects the mechanisms described in models of diabetic nephropathy and retinopathy, where glucose-induced oxidative stress drives mitochondrial dysfunction and eventual cell death[25]. Importantly, while both models converged on mitochondrial damage and caspase activation, only the high-glucose group exhibited sustained NF-κB and FOXO-1 activation, highlighting a unique metabolic stress signature.

The differences in the kinetics between the two models are particularly noteworthy. Staurosporine induced rapid apoptosis, consistent with the acute apoptotic stress typical of cancer therapy models, where tumor cells are exposed to chemotherapeutics under nutrient-deprived conditions[26]. In contrast, high-glucose-induced apoptosis requires a longer exposure time, reflecting the chronic metabolic stress observed in diabetic complications. Thus, this study provides a unique side-by-side demonstration of how apoptosis

can occur via "fast" versus "slow" death programs, depending on the initiating stressor.

Another novel aspect of this study is the comprehensive integration of multiple readouts, including cell viability, ROS generation, mitochondrial depolarization, and gene expression, in a time-resolved manner. Many prior studies have focused on single endpoints, such as ROS or caspase activity, without examining their temporal relationships[27]. By analyzing the 6, 12, and 24 h time points, this study delineated early versus late apoptotic events. For instance, ROS peaked early in the staurosporine model, whereas in the high-glucose model, ROS accumulated progressively, reaching maximal levels at 24 h. Similarly, mitochondrial dysfunction occurred rapidly under serum depletion with staurosporine but was delayed under high glucose levels. These temporal differences emphasize the mechanistic divergence between acute kinase inhibition and chronic metabolic overload.

This study also highlighted unique gene expression signatures. Both models showed upregulation of BAX, CASPASE-9, and p53, consistent with the central role of mitochondrial apoptosis[28]. However, high glucose levels specifically induce RAGE, FOXO-1, and NF-κB, which are strongly implicated in diabetic complications[29]. This finding underscores that while both stressors converge on mitochondrial dysfunction, their upstream regulators are different. The dual observation of shared mitochondrial convergence and differential upstream signaling enhances our understanding of apoptosis in various disease contexts.

The caspase-3/7 activity assay further corroborated the apoptosis-associated responses observed in cell viability, ROS, and mitochondrial membrane potential measurements. The strong, time-dependent increase in caspase activity under serum depletion with staurosporine is consistent with previous reports describing staurosporine as a potent inducer of the mitochondrial apoptotic cascade, leading to cytochrome c release and caspase-9 activation upstream of caspase-3[30]. The observed rapid activation within 6–12 h highlights the acute nature of this model of apoptosis.

In contrast, high-glucose conditions were associated with delayed and modest caspase-3/7 activation, peaking at 24 h. This aligns with studies showing that hyperglycemia induces apoptosis primarily through oxidative stress and AGE-RAGE signaling, which gradually converge on caspase activation[31]. The fact that caspase induction was detectable but weaker than that in the staurosporine group reinforces the interpretation that high glucose levels represent an early-stage hyperglycemia model, reflecting cumulative stress rather than direct kinase inhibition.

It is important to acknowledge the limitations of the caspase-3/7 assay. Although the luminescent DEVDase readout is widely interpreted as caspase-3/7 activity, it may also reflect cleavage by other DEVD-recognising proteases. Furthermore, interpretation must consider normalization approaches, as reductions in viability can artificially inflate the apparent caspase activity per cell. Nonetheless, when combined with MTT, Rhodamine 123, ROS, and gene expression data, the caspase-3/7 assay strengthened the overall evidence that both serum depletion with staurosporine and high-glucose exposure engage apoptosis-associated pathways, albeit with distinct kinetics and magnitudes. These findings confirm that the high-glucose–induced apoptosis model in NRK-52E cells is responsive to intervention with natural products and can therefore be utilised as a screening tool. Berberine, chosen as a reference phytochemical, demonstrated consistent anti-apoptotic activity across multiple endpoints: improved cell viability, preserved mitochondrial function, reduced oxidative stress, suppressed caspase activity, and normalised gene expression.

The observation that berberine mitigates both mitochondrial-dependent apoptosis and glucose-specific stress pathways (RAGE/NF-κB/FOXO) underscores the robustness of this model in capturing physiologically relevant mechanisms of diabetic apoptosis. Previous studies have shown berberine's reno-protective effects in diabetic nephropathy through antioxidant and anti-inflammatory mechanisms, and the present work validates that these effects are detectable within the glucose-induced apoptosis framework. Thus, the inclusion of berberine as a test compound not only strengthens the biological relevance of the glucose-induced apoptosis model but also demonstrates its translational potential for evaluating and screening anti-apoptotic natural products in the context of diabetic complications.

## 5. Conclusion

This study demonstrates that apoptosis in NRK-52E renal epithelial cells proceeds via distinct patterns depending on the inducing stimulus. Serum depletion with staurosporine produced rapid and severe apoptosis characterised by early mitochondrial depolarisation, a sharp ROS burst, and strong caspase activation. In contrast, high-glucose exposure induced a slower but progressive apoptotic response, uniquely associated with RAGE, NF-κB, and FOXO-1 activation, reflecting the metabolic stress conditions relevant to diabetic complications. Importantly, the inclusion of berberine as a proof-of-concept natural product confirmed the responsiveness of the high-glucose model to pharmacological modulation. Berberine significantly improved cell viability, preserved mitochondrial integrity, reduced ROS and caspase activity, and normalised the expression of both mitochondrial apoptotic and glucose-specific stress genes. These findings validate high-glucose–induced apoptosis as a physiologically meaningful *in vitro* model and establish its potential as a screening platform for natural products and therapeutic agents with anti-apoptotic activity in diabetes-related cellular injury.

## 6. Acknowledgements

The authors gratefully acknowledge ARIBAS (Ashok and Rita Patel Institute of Integrated Study and Research in Biotechnology and Allied Sciences), New Vallabh Vidyanagar, for providing laboratory facilities, technical support, and research infrastructure during the course of this study. We also extend our sincere thanks to Sat Kaival Hospital Pvt. Ltd., Lambhvel, Anand, for their invaluable assistance with sample collection, ethical compliance support, and clinical collaboration. Their contributions were instrumental to the successful execution of this study.

## 7. Author Contribution

Conceptualization, Supervision, Project Administration, Funding Acquisition, Writing – Review and Editing, Kinnari Nitin Mistry; Methodology, Investigation, Formal Analysis, Data Curation, Writing – Original Draft. Both the authors have read and agreed to the published version of the manuscript.

## 8. References

1. Maiese K. The impact of ageing and oxidative stress in metabolic and nervous system disorders: programmed cell death and molecular signal transduction crosstalk. Front Immunol. 2023; 14(3):102-107. https://doi.org/10.3389/fimmu.2023.1273570
2. Mosadegh M, Noori Goodarzi N, Erfani Y. A comprehensive insight into apoptosis: molecular mechanisms, signalling pathways, and modulating therapeutics. Cancer Investigation. 2025; 43(1):33-58. https://doi.org/10.1080/07357907.2024.2445528
3. Mustafa M, Ahmad R, Abbas K, Hassan MI, Ahmad W, Habib S, *et al.* Apoptosis: a comprehensive overview of signalling pathways, morphological changes, and physiological significance and therapeutic implications. Cells. 2024; 13(22):1838. https://doi.org/10.3390/cells13221838
4. Zhu S, Zhu Q, Sun X, Zhou J, Zhou Z. ROS accumulation contributes to abamectin-induced apoptosis and autophagy via the inactivation of PI3K/AKT/mTOR pathway in TM3 Leydig cells. J Biochem and Molecular Tox. 2020,10; 34(8). https://doi.org/10.1002/jbt.22505
5. Guo X, Chen KH, Xiao RP, Tang J, Liao H, Guo Y. Mitofusin 2 triggers vascular smooth muscle cell apoptosis via mitochondrial death pathway. Circulation Research. 2007; 101(11):1113-1122. https://doi.org/10.1161/CIRCRESAHA.107.157644
6. Sifuentes-Franco S, Padilla-Tejeda DE, Carrillo-Ibarra S, Miranda-Díaz AG. Oxidative stress, apoptosis, and mitochondrial function in diabetic nephropathy. International Journal of Endocrinology. 2018; 2018(9):1-13. https://doi.org/10.1155/2018/1875870
7. Hu Z, Liu Y, Chen W, Fang W, Wang H, Liang H. Acute glucose fluctuation promotes RAGE expression via reactive oxygen species-mediated NF κB activation in rat podocytes. Mol Med Rep. 2021; 23(5). https://doi.org/10.3892/mmr.2021.11969
8. Parwani K, Mandal P. Role of advanced glycation end products and insulin resistance in diabetic nephropathy. Archives of Physiology and Biochemistry. 2020; 95-107. https://doi.org/10.1080/13813455.2020.1797106
9. Lim C, Zhen AX, Ok S, Fernando PDSM, Herath HMUL, Piao MJ, *et al.* Hesperidin protects sh−sy5y neuronal cells against high glucose−induced apoptosis via regulation of MAPK signalling. Antioxidants. 2022; 11(9):1707. https://doi.org/10.3390/antiox11091707
10. Qin R, Guo L, Xiao F, Zhang L, Lin D. Mst1 deletion reduces hyperglycemia-mediated vascular dysfunction via attenuating mitochondrial fission and modulating the JNK signalling pathway. Journal of Cellular Physiology. 2019; 235(1):294-303. https://doi.org/10.1002/jcp.28969
11. Alnahdi A, John A, Raza H. Augmentation of glucotoxicity, oxidative stress, apoptosis and mitochondrial dysfunction

in HepG2 cells by palmitic acid. Nutrients. 2019; 11(9):1979. https://doi.org/10.3390/nu11091979

12. Soltani A, Pourgheysari B, Shirzad H, Sourani Z. Antiproliferative and apoptosis-inducing activities of thymoquinone in lymphoblastic leukaemia cell line. Indian J Hematol Blood Transfus. 2016; 33(4):516-524. https://doi.org/10.1007/s12288-016-0758-8
13. Azzoz M, Soliman H, Aly S, El-Dabae W, Mounir N, Abdel Shakour N, *et al.* Efficiency of MTT and trypan blue assays for the detection of viability and recovery of different frozen cell lines. Egyptian Journal of Veterinary Sciences. 2024; 55(6):1649-1657. https://doi.org/10.21608/ejvs.2024.260687.1764
14. Breen L, Flynn J, Bergin A, Flampouri E, Butler M. Single cell analysis of Chinese hamster ovary cells during a bioprocess using a novel dynamic imaging system. Biotechnology Progress. 2024; 40(5). https://doi.org/10.1002/btpr.3469
15. Zorova LD, Demchenko EA, Korshunova GA, Tashlitsky VN, Zorov SD, Andrianova NV, *et al.* Is the mitochondrial membrane potential (Δψ) correctly assessed? Intracellular and intramitochondrial modifications of the Δψ probe, rhodamine 123. IJMS. 2022; 23(1):482. https://doi.org/10.3390/ijms23010482
16. Vaneev AN, Klyachko NL, Majouga AG, Korchev YE, Akasov RA, Zhang Y, *et al. In vitro* and i*n vivo* electrochemical measurement of reactive oxygen species after treatment with anticancer drugs. Anal Chem. 2020; 92(12):8010-8014. https://doi.org/10.1021/acs.analchem.0c01256
17. Lederer T, Link A, Kupcinskas J, Hipler NM, Thon C. Comparison of faecal microRNA isolation using various total RNA isolation kits. Genes. 2024; 15(4):498. https://doi.org/10.3390/genes15040498
18. Lins FV, Bispo ECI, Rodrigues NS, Silva MVS, Carvalho JL, Gelfuso GM, *et al.* Ibrutinib modulates proliferation, migration, mitochondrial homeostasis, and apoptosis in melanoma cells. Biomedicines. 2024; 12(5):1012. https://doi.org/10.3390/biomedicines12051012
19. Ran Z, Ma J, Zhang Y, Wen X. Curcumin inhibits high glucose-induced inflammatory injury in human retinal pigment epithelial cells through the ROS PI3K/AKT/mTOR signalling pathway. Mol Med Report. 2018; 19(2). https://doi.org/10.3892/mmr.2018.9749
20. Mahmoudian A, Nokhbatolfoghahaie H, Hakimiha N, Atarbashi-Moghadam F, Azadi A. Effect of fibroblast growth factor 2 and low-level laser therapy on the adhesion and proliferation of periodontal ligament stem cells. J Lasers Med Sci. 2024; 15:e17. https://doi.org/10.34172/jlms.2024.17
21. Shirian FI, Karimi M, Alipour M, Salami S, Nourbakhsh M, Nekufar S, *et al.* Beta-hydroxybutyrate induces lung cancer cell death, mitochondrial impairment and oxidative stress in a long-term glucose-restricted condition. Mol Biol Rep. 2024; 51(1). https://doi.org/10.1007/s11033-024-09501-w
22. Yilmaz O, Jungas T, Ojcius DM, Verbeke P. Activation of the phosphatidylinositol 3-kinase/Akt pathway contributes to survival of primary epithelial cells infected with the periodontal pathogen *Porphyromonas gingivalis*. Infect Immun. 2004; 72(7):3743-3751. https://doi.org/10.1128/IAI.72.7.3743-3751.2004
23. Hamacher-Brady A, Brady NR. Bax/Bak-dependent, Drp1-independent targeting of X-linked inhibitor of apoptosis protein (XIAP) into inner mitochondrial compartments counteracts SMAC/diablo-dependent effector caspase activation. Journal of Biological Chemistry. 2015; 290(36):22005-22018. https://doi.org/10.1074/jbc.M115.643064
24. Horvat A, Vlašić I, Štefulj J, Oršolić N, Jazvinšćak Jembrek M. Flavonols as a Potential Pharmacological Intervention for Alleviating Cognitive Decline in Diabetes: Evidence from Preclinical Studies. Life. 2023; 13(12):2291. https://doi.org/10.3390/life13122291
25. Anastasiou IA, Tentolouris KN, Eleftheriadou I, Tektonidou M, Lambadiari V, Tentolouris N. Effects of advanced glycation end products via oxidative stress on beta cells: insights from *in vitro* and *in vivo* studies and update on emerging therapies. MRMC. 2023; 23(21):2041-2052. https://doi.org/10.2174/1389557523666230510123038
26. Malsy M, Bitzinger D, Bundscherer A, Graf B. Staurosporine induces apoptosis in pancreatic carcinoma cells PaTu 8988t and Panc-1 via the intrinsic signaling pathway. Eur J Med Res. 2019; 24(1). https://doi.org/10.1186/s40001-019-0365-x
27. Zaib S, Khan I, Hayyat A, Ali N, Gul A, Naveed M. Role of mitochondrial membrane potential and lactate dehydrogenase a in apoptosis. ACAMC. 2022; 22(11):2048-2062. https://doi.org/10.2174/1871520621666211126090906
28. Park JH, Seo YH, Jang JH, Jeong CH, Lee S, Park B. Asiatic acid attenuates methamphetamine-induced neuroinflammation and neurotoxicity through blocking of NF-kB/STAT3/ERK and mitochondria-mediated apoptosis pathway. J Neuroinflammation. 2017; 14(1). https://doi.org/10.1186/s12974-017-1009-0
29. Chuah YK, Talib H, Basir R, Nordin N, Tie TH. Receptor for advanced glycation end products and its involvement in inflammatory diseases. International Journal of Inflammation. 2013; 2013(21):1-15. https://doi.org/10.1155/2013/403460
30. Kruman I, Guo Q, Mattson MP. Calcium and reactive oxygen species mediate staurosporine-induced mitochondrial dysfunction and apoptosis in PC12 cells. J Neurosci Res. 1998; 51(3):293-308. https://doi.org/10.1002/(SICI)1097-4547(19980201)51:3<293::AID-JNR3>3.0.CO;2-B
31. Musaogullari A, Mandato A, Chai YC. Role of glutathione depletion and reactive oxygen species generation on caspase-3 activation: a study with the kinase inhibitor staurosporine. Front Physiol. 2020; 11(2). https://doi.org/10.3389/fphys.2020.00998